



This is the accepted manuscript made available via CHORUS. The article has been published as:

Beam Energy Dependence of Fifth- and Sixth-Order Net-Proton Number Fluctuations in $\text{Au} + \text{Au}$ Collisions at RHIC

B. E. Aboona et al. (STAR Collaboration)

Phys. Rev. Lett. **130**, 082301 — Published 24 February 2023

DOI: [10.1103/PhysRevLett.130.082301](https://doi.org/10.1103/PhysRevLett.130.082301)

Beam Energy Dependence of Fifth and Sixth-Order Net-proton Number Fluctuations in Au+Au Collisions at RHIC

B. E. Aboona,¹ J. Adam,² L. Adamczyk,³ J. R. Adams,⁴ I. Aggarwal,⁵ M. M. Aggarwal,⁵ Z. Ahammed,⁶ D. M. Anderson,¹ E. C. Aschenauer,⁷ J. Atchison,⁸ V. Bairathi,⁹ W. Baker,¹⁰ J. G. Ball Cap,¹¹ K. Barish,¹⁰ R. Bellwied,¹¹ P. Bhagat,¹² A. Bhasin,¹² S. Bhatta,¹³ J. Bielcik,² J. Bielcikova,¹⁴ J. D. Brandenburg,⁴ X. Z. Cai,¹⁵ H. Caines,¹⁶ M. Calderón de la Barca Sánchez,¹⁷ D. Cebra,¹⁷ J. Ceska,² I. Chakaberia,¹⁸ P. Chaloupka,² B. K. Chan,¹⁹ Z. Chang,²⁰ D. Chen,¹⁰ J. Chen,²¹ J. H. Chen,²² Z. Chen,²¹ J. Cheng,²³ Y. Cheng,¹⁹ S. Choudhury,²² W. Christie,⁷ X. Chu,⁷ H. J. Crawford,²⁴ M. Csanád,²⁵ G. Dale-Gau,²⁶ A. Das,² M. Daugherty,⁸ I. M. Deppner,²⁷ A. Dhamija,⁵ L. Di Carlo,²⁸ L. Didenko,⁷ P. Dixit,²⁹ X. Dong,¹⁸ J. L. Drachenberg,⁸ E. Duckworth,³⁰ J. C. Dunlop,⁷ J. Engelage,²⁴ G. Eppley,³¹ S. Esumi,³² O. Evdokimov,²⁶ A. Ewigleben,³³ O. Eyser,⁷ R. Fatemi,³⁴ S. Fazio,³⁵ C. J. Feng,³⁶ Y. Feng,³⁷ E. Finch,³⁸ Y. Fisyak,⁷ F. A. Flor,¹⁶ C. Fu,³⁹ C. A. Gagliardi,¹ T. Galatyuk,⁴⁰ F. Geurts,³¹ N. Ghimire,⁴¹ A. Gibson,⁴² K. Gopal,⁴³ X. Gou,²¹ D. Grosnick,⁴² A. Gupta,¹² W. Guryn,⁷ A. Hamed,⁴⁴ Y. Han,³¹ S. Harabasz,⁴⁰ M. D. Harasty,¹⁷ J. W. Harris,¹⁶ H. Harrison,³⁴ W. He,²² X. H. He,⁴⁵ Y. He,²¹ S. Heppelmann,¹⁷ N. Herrmann,²⁷ L. Holub,² C. Hu,⁴⁵ Q. Hu,⁴⁵ Y. Hu,¹⁸ H. Huang,³⁶ H. Z. Huang,¹⁹ S. L. Huang,¹³ T. Huang,²⁶ X. Huang,²³ Y. Huang,²³ Y. Huang,³⁹ T. J. Humanic,⁴ D. Isenhower,⁸ M. Isshiki,³² W. W. Jacobs,²⁰ A. Jalotra,¹² C. Jena,⁴³ A. Jentsch,⁷ Y. Ji,¹⁸ J. Jia,^{7,13} C. Jin,³¹ X. Ju,⁴⁶ E. G. Judd,²⁴ S. Kabana,⁹ M. L. Kabir,¹⁰ S. Kagamaster,³³ D. Kalinkin,^{34,7} K. Kang,²³ D. Kapukchyan,¹⁰ K. Kauder,⁷ H. W. Ke,⁷ D. Keane,³⁰ M. Kelsey,²⁸ Y. V. Khyzhniak,⁴ D. P. Kikoła,⁴⁷ B. Kimelman,¹⁷ D. Kincses,²⁵ I. Kisel,⁴⁸ A. Kiselev,⁷ A. G. Knospe,³³ H. S. Ko,¹⁸ L. K. Kosarzewski,² L. Kramarik,² L. Kumar,⁵ S. Kumar,⁴⁵ R. Kunnawalkam Elayavalli,¹⁶ R. Lacey,¹³ J. M. Landgraf,⁷ J. Lauret,⁷ A. Lebedev,⁷ J. H. Lee,⁷ Y. H. Leung,²⁷ N. Lewis,⁷ C. Li,²¹ C. Li,⁴⁶ W. Li,³¹ X. Li,⁴⁶ Y. Li,⁴⁶ Y. Li,²³ Z. Li,⁴⁶ X. Liang,¹⁰ Y. Liang,³⁰ R. Licenik,^{14,2} T. Lin,²¹ M. A. Lisa,⁴ C. Liu,⁴⁵ F. Liu,³⁹ H. Liu,²⁰ H. Liu,³⁹ L. Liu,³⁹ T. Liu,¹⁶ X. Liu,⁴ Y. Liu,¹ Z. Liu,³⁹ T. Ljubicic,⁷ W. J. Llope,²⁸ O. Lomicky,² R. S. Longacre,⁷ E. Loyd,¹⁰ T. Lu,⁴⁵ N. S. Lukow,⁴¹ X. F. Luo,³⁹ L. Ma,²² R. Ma,⁷ Y. G. Ma,²² N. Magdy,¹³ D. Mallick,⁴⁹ S. Margetis,³⁰ C. Markert,⁵⁰ H. S. Matis,¹⁸ J. A. Mazer,⁵¹ G. McNamara,²⁸ K. Mi,³⁹ S. Mioduszewski,¹ B. Mohanty,⁴⁹ I. Mooney,¹⁶ A. Mukherjee,²⁵ M. I. Nagy,²⁵ A. S. Nain,⁵ J. D. Nam,⁴¹ Md. Nasim,²⁹ D. Neff,¹⁹ J. M. Nelson,²⁴ D. B. Nemes,¹⁶ M. Nie,²¹ T. Niida,³² R. Nishitani,³² T. Nonaka,³² A. S. Nunes,⁷ G. Odyniec,¹⁸ A. Ogawa,⁷ S. Oh,¹⁸ K. Okubo,³² B. S. Page,⁷ R. Pak,⁷ J. Pan,¹ A. Pandav,⁴⁹ A. K. Pandey,⁴⁵ T. Pani,⁵¹ A. Paul,¹⁰ B. Pawlik,⁵² D. Pawlowska,⁴⁷ C. Perkins,²⁴ J. Pluta,⁴⁷ B. R. Pokhrel,⁴¹ M. Posik,⁴¹ T. Protzman,³³ V. Prozorova,² N. K. Pruthi,⁵ M. Przybycien,³ J. Putschke,²⁸ Z. Qin,²³ H. Qiu,⁴⁵ A. Quintero,⁴¹ C. Racz,¹⁰ S. K. Radhakrishnan,³⁰ N. Raha,²⁸ R. L. Ray,⁵⁰ R. Reed,³³ H. G. Ritter,¹⁸ C. W. Robertson,³⁷ M. Robotkova,^{14,2} J. L. Romero,¹⁷ M. A. Rosales Aguilar,³⁴ D. Roy,⁵¹ P. Roy Chowdhury,⁴⁷ L. Ruan,⁷ A. K. Sahoo,²⁹ N. R. Sahoo,²¹ H. Sako,³² S. Salur,⁵¹ S. Sato,³² W. B. Schmidke,⁷ N. Schmitz,⁵³ F.-J. Seck,⁴⁰ J. Seger,⁵⁴ R. Seto,¹⁰ P. Seyboth,⁵³ N. Shah,⁵⁵ P. V. Shanmuganathan,⁷ M. Shao,⁴⁶ T. Shao,²² M. Sharma,¹² N. Sharma,²⁹ R. Sharma,⁴³ S. R. Sharma,⁴³ A. I. Sheikh,³⁰ D. Y. Shen,²² K. Shen,⁴⁶ S. S. Shi,³⁹ Y. Shi,²¹ Q. Y. Shou,²² F. Si,⁴⁶ J. Singh,⁵ S. Singha,⁴⁵ P. Sinha,⁴³ M. J. Skoby,^{56,37} N. Smirnov,¹⁶ Y. Söhngen,²⁷ Y. Song,¹⁶ B. Srivastava,³⁷ T. D. S. Stanislaus,⁴² M. Stefaniak,⁴ D. J. Stewart,²⁸ B. Stringfellow,³⁷ Y. Su,⁴⁶ A. A. P. Suaide,⁵⁷ M. Sumbera,¹⁴ C. Sun,¹³ X. Sun,⁴⁵ Y. Sun,⁴⁶ Y. Sun,⁵⁸ B. Surrow,⁴¹ Z. W. Sweger,¹⁷ P. Szymanski,⁴⁷ A. Tamis,¹⁶ A. H. Tang,⁷ Z. Tang,⁴⁶ T. Tarnowsky,⁵⁹ J. H. Thomas,¹⁸ A. R. Timmins,¹¹ D. Tlusty,⁵⁴ T. Todoroki,³² C. A. Tomkiel,³³ S. Trentalange,¹⁹ R. E. Tribble,¹ P. Tribedy,⁷ T. Truhlar,² B. A. Trzeciak,² O. D. Tsai,^{19,7} C. Y. Tsang,^{30,7} Z. Tu,⁷ T. Ullrich,⁷ D. G. Underwood,^{60,42} I. Upsal,³¹ G. Van Buren,⁷ J. Vanek,⁷ I. Vassiliev,⁴⁸ V. Verkest,²⁸ F. Videbæk,⁷ S. A. Voloshin,²⁸ F. Wang,³⁷ G. Wang,¹⁹ J. S. Wang,⁵⁸ X. Wang,²¹ Y. Wang,⁴⁶ Y. Wang,³⁹ Y. Wang,²³ Z. Wang,²¹ J. C. Webb,⁷ P. C. Weidenkaff,²⁷ G. D. Westfall,⁵⁹ D. Wielanek,⁴⁷ H. Wieman,¹⁸ G. Wilks,²⁶ S. W. Wissink,²⁰ R. Witt,⁶¹ J. Wu,³⁹ J. Wu,⁴⁵ X. Wu,¹⁹ Y. Wu,¹⁰ B. Xi,¹⁵ Z. G. Xiao,²³ W. Xie,³⁷ H. Xu,⁵⁸ N. Xu,¹⁸ Q. H. Xu,²¹ Y. Xu,²¹ Y. Xu,³⁹ Z. Xu,⁷ Z. Xu,¹⁹ G. Yan,²¹ Z. Yan,¹³ C. Yang,²¹ Q. Yang,²¹ S. Yang,⁶² Y. Yang,³⁶ Z. Ye,³¹ Z. Ye,²⁶ L. Yi,²¹ K. Yip,⁷ Y. Yu,²¹ H. Zbroszczyk,⁴⁷ W. Zha,⁴⁶ C. Zhang,¹³ D. Zhang,³⁹ J. Zhang,²¹ S. Zhang,⁴⁶ X. Zhang,⁴⁵ Y. Zhang,⁴⁵ Y. Zhang,⁴⁶ Y. Zhang,³⁹ Z. J. Zhang,³⁶ Z. Zhang,⁷ Z. Zhang,²⁶ F. Zhao,⁴⁵ J. Zhao,²² M. Zhao,⁷ C. Zhou,²² J. Zhou,⁴⁶ S. Zhou,³⁹ Y. Zhou,³⁹ X. Zhu,²³ M. Zurek,⁶⁰ and M. Zyzak⁴⁸

(STAR Collaboration)

¹Texas A&M University, College Station, Texas 77843

²Czech Technical University in Prague, FNSPE, Prague 115 19, Czech Republic

³AGH University of Science and Technology, FPACS, Cracow 30-059, Poland

- 52 ⁴Ohio State University, Columbus, Ohio 43210
53 ⁵Panjab University, Chandigarh 160014, India
54 ⁶Variable Energy Cyclotron Centre, Kolkata 700064, India
55 ⁷Brookhaven National Laboratory, Upton, New York 11973
56 ⁸Abilene Christian University, Abilene, Texas 79699
57 ⁹Instituto de Alta Investigación, Universidad de Tarapacá, Arica 1000000, Chile
58 ¹⁰University of California, Riverside, California 92521
59 ¹¹University of Houston, Houston, Texas 77204
60 ¹²University of Jammu, Jammu 180001, India
61 ¹³State University of New York, Stony Brook, New York 11794
62 ¹⁴Nuclear Physics Institute of the CAS, Rez 250 68, Czech Republic
63 ¹⁵Shanghai Institute of Applied Physics, Chinese Academy of Sciences, Shanghai 201800
64 ¹⁶Yale University, New Haven, Connecticut 06520
65 ¹⁷University of California, Davis, California 95616
66 ¹⁸Lawrence Berkeley National Laboratory, Berkeley, California 94720
67 ¹⁹University of California, Los Angeles, California 90095
68 ²⁰Indiana University, Bloomington, Indiana 47408
69 ²¹Shandong University, Qingdao, Shandong 266237
70 ²²Fudan University, Shanghai, 200433
71 ²³Tsinghua University, Beijing 100084
72 ²⁴University of California, Berkeley, California 94720
73 ²⁵ELTE Eötvös Loránd University, Budapest, Hungary H-1117
74 ²⁶University of Illinois at Chicago, Chicago, Illinois 60607
75 ²⁷University of Heidelberg, Heidelberg 69120, Germany
76 ²⁸Wayne State University, Detroit, Michigan 48201
77 ²⁹Indian Institute of Science Education and Research (IISER), Berhampur 760010, India
78 ³⁰Kent State University, Kent, Ohio 44242
79 ³¹Rice University, Houston, Texas 77251
80 ³²University of Tsukuba, Tsukuba, Ibaraki 305-8571, Japan
81 ³³Lehigh University, Bethlehem, Pennsylvania 18015
82 ³⁴University of Kentucky, Lexington, Kentucky 40506-0055
83 ³⁵University of Calabria & INFN-Cosenza, Italy
84 ³⁶National Cheng Kung University, Tainan 70101
85 ³⁷Purdue University, West Lafayette, Indiana 47907
86 ³⁸Southern Connecticut State University, New Haven, Connecticut 06515
87 ³⁹Central China Normal University, Wuhan, Hubei 430079
88 ⁴⁰Technische Universität Darmstadt, Darmstadt 64289, Germany
89 ⁴¹Temple University, Philadelphia, Pennsylvania 19122
90 ⁴²Valparaiso University, Valparaiso, Indiana 46383
91 ⁴³Indian Institute of Science Education and Research (IISER) Tirupati, Tirupati 517507, India
92 ⁴⁴American University of Cairo, New Cairo 11835, New Cairo, Egypt
93 ⁴⁵Institute of Modern Physics, Chinese Academy of Sciences, Lanzhou, Gansu 730000
94 ⁴⁶University of Science and Technology of China, Hefei, Anhui 230026
95 ⁴⁷Warsaw University of Technology, Warsaw 00-661, Poland
96 ⁴⁸Frankfurt Institute for Advanced Studies FIAS, Frankfurt 60438, Germany
97 ⁴⁹National Institute of Science Education and Research, HBNI, Jatni 752050, India
98 ⁵⁰University of Texas, Austin, Texas 78712
99 ⁵¹Rutgers University, Piscataway, New Jersey 08854
100 ⁵²Institute of Nuclear Physics PAN, Cracow 31-342, Poland
101 ⁵³Max-Planck-Institut für Physik, Munich 80805, Germany
102 ⁵⁴Creighton University, Omaha, Nebraska 68178
103 ⁵⁵Indian Institute Technology, Patna, Bihar 801106, India
104 ⁵⁶Ball State University, Muncie, Indiana, 47306
105 ⁵⁷Universidade de São Paulo, São Paulo, Brazil 05314-970
106 ⁵⁸Huzhou University, Huzhou, Zhejiang 313000
107 ⁵⁹Michigan State University, East Lansing, Michigan 48824
108 ⁶⁰Argonne National Laboratory, Argonne, Illinois 60439
109 ⁶¹United States Naval Academy, Annapolis, Maryland 21402
110 ⁶²South China Normal University, Guangzhou, Guangdong 510631
111 (Dated: January 11, 2023)

112 We report the beam energy and collision centrality dependence of fifth and sixth order cumulants
113 (C_5 , C_6) and factorial cumulants (κ_5 , κ_6) of net-proton and proton number distributions, from
114 center-of-mass energy ($\sqrt{s_{NN}}$) 3 GeV to 200 GeV Au+Au collisions at RHIC. Cumulant ratios of

net-proton (taken as proxy for net-baryon) distributions generally follow the hierarchy expected from QCD thermodynamics, except for the case of collisions at 3 GeV. The measured values of C_6/C_2 for 0-40% centrality collisions show progressively negative trend with decreasing energy, while it is positive for the lowest energy studied. These observed negative signs are consistent with QCD calculations (for baryon chemical potential, $\mu_B \leq 110$ MeV) which contains the crossover transition range. In addition, for energies above 7.7 GeV, the measured proton κ_n , within uncertainties, does not support the two-component (Poisson+Binomial) shape of proton number distributions that would be expected from a first-order phase transition. Taken in combination, the hyper-order proton number fluctuations suggest that the structure of QCD matter at high baryon density, $\mu_B \sim 750$ MeV at $\sqrt{s_{NN}} = 3$ GeV is starkly different from those at vanishing $\mu_B \sim 24$ MeV at $\sqrt{s_{NN}} = 200$ GeV and higher collision energies.

An important goal of heavy-ion physics is to study the phase structure of strongly interacting matter. The diagram of such strongly-interacting matter, known as the Quantum Chromodynamics (QCD) phase diagram, shows the phase structure as a function of temperature (T) and baryon chemical potential (μ_B) [1, 2]. Lattice QCD (LQCD) calculations have established the quark-hadron phase transition as a smooth crossover at vanishing μ_B [3]. At large μ_B , QCD-based model calculations indicate that the crossover is replaced by a first-order transition [4, 5] which terminates at a critical point.

Varying the collision energy of heavy nuclei results in a variation in T and μ_B of the strongly-interacting system produced in these collisions, allowing an experimental study of the QCD phase diagram [6]. Event-by-event fluctuations or cumulants of net-particle number (N) distributions in heavy-ion collisions are sensitive observables for this study [7–10]. The cumulants are extensive quantities that can be used to characterize the shape of a distribution. The fifth and sixth-order cumulants, relevant to the current study, are defined as follows: $C_5 = \langle \delta N^5 \rangle - 10 \langle \delta N^3 \rangle \langle \delta N^2 \rangle$ and $C_6 = \langle \delta N^6 \rangle - 15 \langle \delta N^4 \rangle \langle \delta N^2 \rangle - 10 \langle \delta N^3 \rangle^2 + 30 \langle \delta N^2 \rangle^3$, where $\delta N = N - \langle N \rangle$ (For details see Supplemental Material [11]). For a thermalized system, the ratio of cumulants are directly linked to the susceptibilities (χ_n) calculated in a fixed volume, as done in lattice QCD, and in QCD-based and thermal models [12–15]. Experimental measurement of higher order cumulants are also important to understand thermalization in high energy nuclear collisions where the size and duration of the medium is limited [16]. The cumulants, up to the fourth order of various net-particle multiplicity distributions have been analyzed from the first phase of the beam energy scan (BES) program at the Relativistic Heavy-Ion Collider (RHIC) facility [17–24] and by the HADES experiment at GSI [25]. The fourth-to-second order cumulant ratio, C_4/C_2 , of net-proton number distributions from the Solenoidal Tracker at RHIC (STAR) experiment shows a non-monotonic collision energy dependence that is qualitatively consistent with expectations from a critical point in the QCD phase diagram [19].

Up to the fourth-order net-proton cumulant ratios, the experimental measurements are positive [19] which is re-

produced by several model calculations. These include calculations with a crossover quark-hadron transition such as the LQCD [26] and the QCD-based functional renormalization group (FRG) model [27], and those without any phase transition effects like the hadronic transport model UrQMD [28] and the thermal hadron resonance gas (HRG) model [15]. Only after extending the order of fluctuations to five and six (also called hyper-orders) do the theoretical calculations with and without QCD phase transitions show a difference in sign. Negative sign of baryon number susceptibility ratios, χ_5^B/χ_1^B and χ_6^B/χ_2^B (also called hyper-skewness and hyper-kurtosis, respectively) is predicted by LQCD [26, 29] near the quark-hadron transition temperature for $\mu_B \leq 110$ MeV. The FRG calculations also yield negative χ_5^B/χ_1^B and χ_6^B/χ_2^B over a wide μ_B range 24 – 420 MeV corresponding to central Au+Au collisions at $\sqrt{s_{NN}} = 200 - 7.7$ GeV [27]. Additionally, a particular ordering of susceptibility ratios: $\chi_3^B/\chi_1^B > \chi_4^B/\chi_2^B > \chi_5^B/\chi_1^B > \chi_6^B/\chi_2^B$ is predicted by LQCD [26]. This is in contrast to the HRG model predictions with an ideal gas equation of state in a grand canonical ensemble framework which remain positive at unity for all ratios [29].

In search of the first-order phase transition, the factorial cumulants of proton multiplicity distributions have been suggested [30]. Factorial cumulants, κ_n , up to the sixth order can be defined in terms of cumulants [31] as $\kappa_1 = C_1$, $\kappa_2 = -C_1 + C_2$, $\kappa_3 = 2C_1 - 3C_2 + C_3$, $\kappa_4 = -6C_1 + 11C_2 - 6C_3 + C_4$, $\kappa_5 = 24C_1 - 50C_2 + 35C_3 - 10C_4 + C_5$ and $\kappa_6 = -120C_1 + 274C_2 - 225C_3 + 85C_4 - 15C_5 + C_6$. The presence of a mixed phase in a first-order phase transition results in a bimodal or two-component structure in the proton multiplicity distribution. Such a bimodal distribution, modeled as Poisson+Binomial distributions, yields large factorial cumulants which increase in magnitude and alternate in sign with increasing order [30, 32]. In probing the two-component nature, the factorial cumulants are less demanding statistically and are more sensitive than regular cumulants [30].

The work reported in this letter is intended to identify the nature of the phase transition over a wide range in μ_B by examining the sign of the hyper-order fluctuations. A recent study of net-proton sixth-order cumulants by STAR hints at a crossover in Au+Au collisions

TABLE I. Total event statistics (in millions) in Au+Au collisions for various collision energies ($\sqrt{s_{NN}}$).

$\sqrt{s_{NN}}$ (GeV)	3	7.7	11.5	14.5	19.6	27	39	54.4	62.4	200
Events	140	3	6.6	20	15	30	86	550	47	900

at $\sqrt{s_{NN}} = 200$ GeV ($\mu_B \approx 20$ MeV) [33]. In this work, we present new data down to the lowest energy accessible by STAR ($\sqrt{s_{NN}} = 3$ GeV and $\mu_B \approx 750$ MeV), along with the measurements of fifth-order net-proton cumulants and fifth- and sixth-order proton factorial cumulants.

The data from Au+Au collisions having signals in trigger detectors [34, 35] above a noise threshold (called minimum bias) at ten collision energies from $\sqrt{s_{NN}} = 3$ to 200 GeV from the STAR BES-I and fixed-target (FXT) program were analyzed. The number of analyzed events at each energy is summarized in Table I. The 3 GeV collision data were collected in FXT mode with a constraint on the interaction point (also known as the primary vertex) along the beam axis (V_z) of $199.5 < V_z < 202$ cm, and the remaining energies were taken in the collider mode of detector operation with V_z within ± 30 cm from the center of the STAR detector except for 7.7 GeV data, where ± 40 cm was used [20, 36]. The tracking and particle identification (PID) are carried out using time projection chamber (TPC) and time of flight (TOF) detectors [37]. Protons and antiprotons are required to have rapidity $|y| < 0.5$ at collider energies, and $-0.5 < y < 0$ at 3 GeV due to the asymmetric detector acceptance in the fixed-target mode. The distance of closest approach (DCA) of the (anti-)proton tracks to the primary vertex is required to be less than 1 cm to suppress background [18]. The transverse momentum criterion of $0.4 < p_T < 2.0$ GeV/c is applied at all energies. A variable $n\sigma$ [21] that quantifies, in terms of standard deviation, the difference between measured dE/dx from the TPC and its expected value for protons [38] is utilized for proton identification. We used $|n\sigma| < 2$. In addition, mass squared (m^2) measured using the TOF detector is required to satisfy $0.6 < m^2 < 1.2$ GeV²/c⁴ in the p_T range $0.8 < p_T < 2.0$ GeV/c to achieve high purity for protons [20]. For FXT energy at 3 GeV, PID using both TPC and TOF is shown in panel (a) of Fig. 1. At this energy, if momentum $p \leq 2$ GeV/c, only the TPC is used for PID; otherwise, both TPC and TOF are used. The purity of protons in the selected kinematic space is higher than 95% at all energies [19]. Centrality is determined using the charged-particle multiplicity measured by the TPC, excluding protons and anti-protons to avoid self-correlations. Results from 0-40% and 50-60% centrality classes are reported. Pile-up events, which happen when separate collisions are reconstructed as a single event, are removed from the analysis by examining the correlation between multiplicities registered in the TPC and

TOF [19, 33]. Additionally, at higher energies, $\sqrt{s_{NN}} > 27$ GeV, information from a vertex position detector is used for removing pileup events [20]. Due to higher collision rates with the FXT configuration, the pile-up effect becomes large compared to that in collider mode. The correction of cumulants for this effect is then done following the method suggested in Ref. [39].

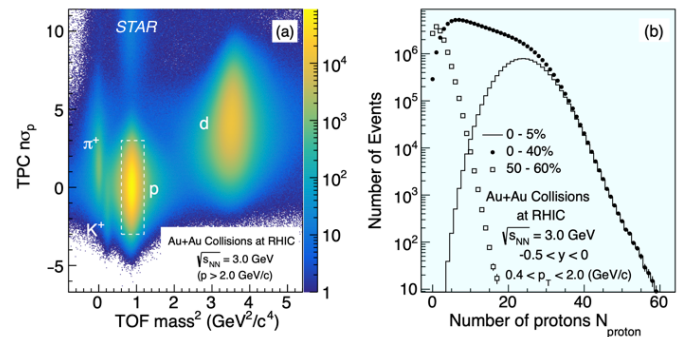


FIG. 1. (a) Particle identification using $n\sigma_p$ (TPC) versus m^2 (TOF) for Au+Au minimum bias collisions at 3 GeV (FXT). A momentum criterion $p > 2$ GeV/c is applied when using m^2 for proton PID. (b) Proton multiplicity distributions from three collision centralities. These distributions are not corrected for detector efficiency and pile-up effects.

Panel (b) of Fig 1 shows proton multiplicity distributions for 0-5%, 0-40% and 50-60% collision centralities for Au+Au collisions at 3 GeV. Because the number of anti-protons is negligible at this energy (less than the number of protons by 6 orders of magnitude [40]), cumulants of proton distributions are calculated instead of net-proton distributions. Cumulants are then corrected for finite detector efficiency assuming binomial detector response [41–47]. In previous work, relaxing the binomial assumption and implementing an unfolding-based correction for cumulants up to the sixth order for Au+Au collisions at $\sqrt{s_{NN}} = 200$ GeV yielded values consistent with an analytical binomial correction formula within uncertainties [19, 33]. To suppress the initial-volume fluctuation effects on cumulants for a given centrality, a centrality bin width correction (CBWC) is performed [48]. While Monte-Carlo studies have shown that at low multiplicities and lower energies residual volume fluctuation effects may remain, the magnitude of the additional correction is highly model dependent [40, 49]. Further theoretical understanding of these residual effects are clearly needed before applying to the data and therefore in this analysis only the CBWC is performed. From cumulants, we construct the factorial cumulants and ratios of cumulants which are the observables of this work. The statistical uncertainties on these observables are estimated using the bootstrap method [43, 50, 51]. Systematic uncertainties are estimated by varying track selection, particle identification criteria, background estimates (DCA), and track reconstruction efficiency.

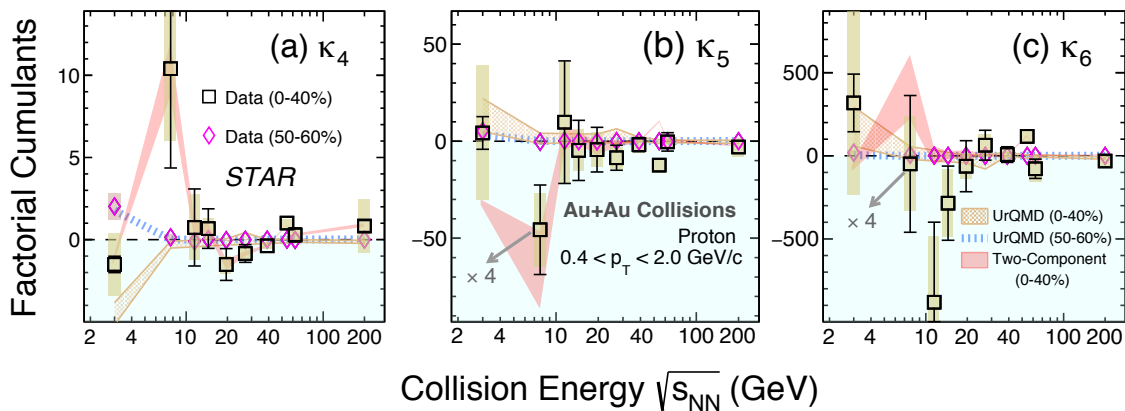


FIG. 2. κ_4 (a), κ_5 (b), κ_6 (c) of proton distribution in Au+Au collisions from 3 GeV to 200 GeV. The results are shown for 0-40% (squares) and 50-60% (diamonds) centralities. The bars and bands on the data points represent the statistical and systematic uncertainties, respectively. The Two-Component Model (0-40%) and UrQMD model (0-40% and 50-60%) calculations are shown as red, brown bands and blue dashed lines, respectively. The Two-Component Model (with Binomial and Poissonian distributions as constituent components) requires κ_n up to the fourth order as inputs to predict κ_5 and κ_6 . Uncertainties are statistical for the model calculations. The κ_5 and κ_6 data at 7.7 GeV (0-40%) are scaled down by a factor of 4 for clarity of presentation.

303 Figure 2 shows collision energy dependence of proton
 304 factorial cumulants, κ_4 , κ_5 and κ_6 for 0-40% and 50-60%
 305 centralities. At 7.7 GeV, large positive κ_4 and negative
 306 κ_5 are observed for 0-40% collisions, albeit with large un-
 307 certainties. In contrast, at higher energies, the factorial
 308 cumulants of all orders show small deviations from zero
 309 and from UrQMD expectations. UrQMD calculations
 310 reproduce the 3 GeV measurements. The energy depen-
 311 dence trend of the κ_5 and κ_6 measurements is largely re-
 312 produced by calculations from a Two-Component Model
 313 for proton multiplicity, motivated by the assumption of
 314 a first-order phase transition, which inputs in its con-
 315 struction the experimental data of κ_n up to the fourth
 316 order and predicts κ_5 and κ_6 [30, 32] (see Supplemen-
 317 tal Material [11] for details). Vanishing values of fac-
 318 torial cumulants would imply that only the Poissonian
 319 part of the Two-Component Model survives. The small
 320 deviation from zero observed for the proton κ_n and the
 321 absence of a sign change with increasing order for ener-
 322 gies above 7.7 GeV within uncertainties does not support
 323 the two-component structure for the proton multiplicity
 324 distributions at those energies. Note that at 54.4 GeV,
 325 a sign change is observed with increasing order for the
 326 three factorial cumulants at a level of $2.5 - 3 \sigma_{\text{tot}}$ (σ_{tot}
 327 is the statistical and systematic uncertainties added in
 328 quadrature). However the Two-Component Model cal-
 329 culation does not show such a trend. The peripheral 50-
 330 60% measurements are either positive or consistent with
 331 zero within uncertainties at all energies.

332 As proxies for net-baryon cumulant ratios [42], C_4/C_2 ,
 333 C_5/C_1 and C_6/C_2 of net-proton distributions in Au+Au
 334 collisions from 3 GeV to 200 GeV for 0-40% and 50-60%
 335 centralities are presented in Fig. 3. C_4/C_2 for 0-40%
 336 centrality is positive at all energies. Various model cal-

culations presented for C_4/C_2 are also positive. C_5/C_1
 for 0-40% centrality exhibits weak collision energy
 dependence and fluctuates about zero with $\lesssim 2.2\sigma_{\text{tot}}$
 significance except at 3 GeV where it has a large positive
 value. C_6/C_2 for the same centrality is increasingly
 negative from higher to lower energies down to 7.7 GeV
 and becomes positive at 3 GeV. The deviations of C_6/C_2
 from zero at all the energies are within $1.7\sigma_{\text{tot}}$. When
 interpreting the 3 GeV data, one should keep in mind that
 the initial volume fluctuation effects become significant
 due to lower charged particle multiplicity. The increas-
 ingly negative sign of C_6/C_2 with decreasing energy in
 the range 7.7 GeV to 200 GeV is qualitatively consist-
 ent with LQCD and FRG calculations that include a
 crossover quark-hadron transition, subject to caveats dis-
 cussed in Ref. [33]. The overall significance of observing
 negative C_6/C_2 in more than half of the collision ener-
 gies in the range 7.7 GeV to 200 GeV is found to be 1.7σ
 (see Supplemental Material [11]). The UrQMD expecta-
 tions for these two ratios are either positive or consistent
 with zero within uncertainties. Expectations from HRG
 CE are positive for energies greater than 19.6 GeV and
 become negative only for lower energies (see Supplemental
 Material [11] for an enlarged view of model calculations).
 Recent hydrodynamic calculations also show a similar
 energy dependence trend as HRG CE [53]. All three
 ratios are non-negative for peripheral 50-60% centrality
 and qualitatively consistent with UrQMD expectations.
 As the event statistics are lowest at 7.7 GeV (1.2 million
 events in 0-40% centrality) among all energies, within the
 current statistical limitations, the robustness of the neg-
 ative sign of C_6/C_2 at 7.7 GeV (0-40%) was verified
 by performing a study on K-statistics [54] (also known as
 unbiased estimators of a population's cumulants) and on

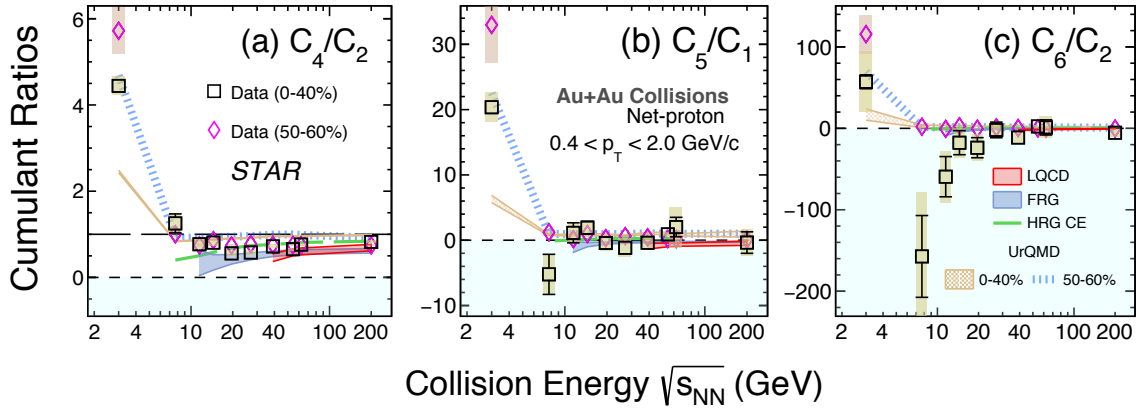


FIG. 3. C_4/C_2 (a), C_5/C_1 (b) and C_6/C_2 (c) of the net-proton distribution in Au+Au collisions from 3 GeV to 200 GeV. The results are shown for 0-40% (squares) and 50-60% (diamonds) centralities. The bars and bands on the data points represent the statistical and systematic uncertainties, respectively. LQCD (39 – 200 GeV) [26], FRG (11.5 – 200 GeV) [27], UrQMD (0-40%, 50-60%), and HRG model calculations (7.7 – 200 GeV) with canonical ensemble [52] (HRG CE) are shown as red, grey, brown bands, blue and green dashed lines, respectively.

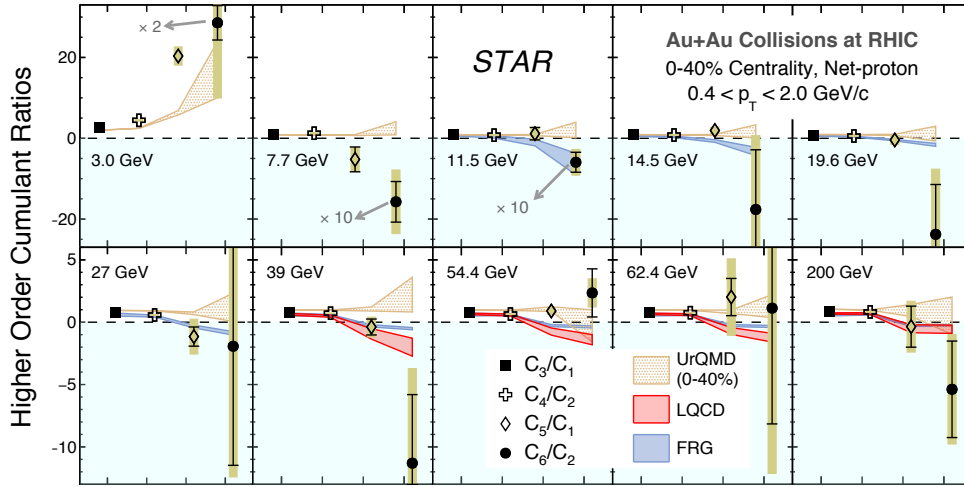


FIG. 4. C_3/C_1 (filled square), C_4/C_2 (open cross), C_5/C_1 (open diamond) and C_6/C_2 (filled circle) of net-proton distributions in 0-40% Au+Au collisions from 3 GeV to 200 GeV. The bars and bands on the data points represent the statistical and systematic uncertainties, respectively. LQCD (39 – 200 GeV) [26], FRG (11.5 – 200 GeV) [27] and UrQMD calculations (0-40% centrality) are shown as red, blue and brown bands respectively. The C_6/C_2 data at 3 GeV (7.7 and 11.5 GeV) are scaled down by a factor of 2 (10) for clarity of presentation.

371 the sample size dependence of net-proton C_6/C_2 which³⁸⁴
 372 involved creating random samples of varying event statis-³⁸⁵
 373 tics from 7.7 GeV data (see Supplemental Material [11]).³⁸⁶
 374 Measurements of the three ratios at collider energies us-³⁸⁷
 375 ing the same rapidity acceptance as for 3 GeV FXT data,³⁸⁸
 376 i.e., $-0.5 < y < 0$, yield similar conclusions regarding the³⁸⁹
 377 sign as reported here (see Supplemental Material [11]).³⁹⁰

378 A particular ordering of net-baryon cumulant ratios:³⁹²
 379 $C_3/C_1 > C_4/C_2 > C_5/C_1 > C_6/C_2$, predicted by LQCD³⁹³
 380 was subjected to experimental verification in Fig. 4.³⁹⁴
 381 Within uncertainties, the measurements for 0-40% cen-³⁹⁵
 382 trality in the energy range 7.7 GeV to 200 GeV are³⁹⁶
 383 consistent with the ordering expected from LQCD (al-

though at 54.4 and 62.4 GeV, the hierarchy is not as
 clear as at other energies). While the FRG calculations
 also follow the predicted hierarchy, the UrQMD
 calculations within uncertainties do not show any clear
 ordering and remain non-negative at all energies. At
 3 GeV the cumulant ratios show a reverse ordering:
 $C_3/C_1 < C_4/C_2 < C_5/C_1 < C_6/C_2$. The probability
 that the higher energy data would follow a 3 GeV ordering
 varies between 0.14 – 10% (see Supplemental Mate-
 rial [11]). The ordering observed at 3 GeV is reproduced
 by UrQMD calculations. These observations suggest that
 the interactions are dominantly hadronic at 3 GeV. Re-
 cent results by the STAR experiment on proton C_4/C_2

showing suppression at 3 GeV for central 0-5% Au+Au collisions also supports this inference, indicating that a possible critical point could only exist at collision energies higher than 3 GeV [40].

In conclusion, measurements of net-proton C_5/C_1 and C_6/C_2 and proton κ_5 and κ_6 are reported in Au+Au collisions over a broad range of collision energies from 3 GeV to 200 GeV corresponding to a μ_B range of 750 MeV to 24 MeV. The data are presented for 0-40% and 50-60% collision centralities. For the first time, we test the ordering of cumulant ratios $C_3/C_1 > C_4/C_2 > C_5/C_1 > C_6/C_2$ expected from QCD thermodynamics. While the overall all measured trend for cumulant ratios from 7.7 GeV to 200 GeV seem to follow this hierarchy, a reverse ordering is seen at 3 GeV. C_6/C_2 for 0-40% centrality is increasingly negative with decreasing energy, except at 3 GeV where it is positive. Their deviations from zero at each energy are within $1.7\sigma_{\text{tot}}$. The significance of finding negative C_6/C_2 (0-40%) at more than half of the collision energies over the range 7.7 GeV to 200 GeV was found to be 1.7σ . The negative sign of C_6/C_2 is consistent with QCD calculations ($\mu_B \leq 110$ MeV) that include a crossover quark-hadron transition. In contrast, the peripheral 50-60% data, and calculations from the UrQMD model which does not include any QCD transition, are either positive or consistent with zero.

Proton factorial cumulants $\kappa_4, \kappa_5, \kappa_6$ (0-40%) are presented as sensitive observables to probe a possible first-order phase transition [30]. The measurements indicate the possibility of a sign change at low collision energies, although the uncertainties are large. For energies above 7.7 GeV, the measured proton κ_n within uncertainties do not support the two-component (Poisson+Binomial) shape of proton distributions that is expected from a first-order phase transition. Peripheral 50-60% data do not show a sign change with increasing order and are consistent with calculations from the UrQMD model at all energies. The agreement between the presented data and UrQMD at 3 GeV suggests that matter is predominantly hadronic at such low collision energies. Taken together, the hyper-order proton number fluctuations suggest that the structure of QCD matter at high baryon density, $\mu_B \sim 750$ MeV at $\sqrt{s_{NN}} = 3$ GeV is starkly different from those at vanishing $\mu_B \sim 24$ MeV at $\sqrt{s_{NN}} = 200$ GeV and higher collision energies. Precision measurements in BES-II with large event statistics will be necessary to confirm these observations.

We thank the RHIC Operations Group and RCF at BNL, the NERSC Center at LBNL, and the Open Science Grid consortium for providing resources and support. This work was supported in part by the Office of Nuclear Physics within the U.S. DOE Office of Science, the U.S. National Science Foundation, National Natural Science Foundation of China, Chinese Academy of Science, the Ministry of Science and Technology of China and the Chinese Ministry of Education, the Higher Education

Sprout Project by Ministry of Education at NCKU, the National Research Foundation of Korea, Czech Science Foundation and Ministry of Education, Youth and Sports of the Czech Republic, Hungarian National Research, Development and Innovation Office, New National Excellence Programme of the Hungarian Ministry of Human Capacities, Department of Atomic Energy and Department of Science and Technology of the Government of India, the National Science Centre and WUT ID-UB of Poland, the Ministry of Science, Education and Sports of the Republic of Croatia, German Bundesministerium für Bildung, Wissenschaft, Forschung and Technologie (BMBF), Helmholtz Association, Ministry of Education, Culture, Sports, Science, and Technology (MEXT) and Japan Society for the Promotion of Science (JSPS).

-
- [1] K. Rajagopal and F. Wilczek, “The Condensed matter physics of QCD,” in *At the frontier of particle physics. Handbook of QCD*. Vol. 1-3, pp. 2061-2151
 - [2] A. Bzdak, S. Esumi, V. Koch, J. Liao, M. Stephanov and N. Xu, *Phys. Rept.* **853**, 1-87 (2020)
 - [3] Y. Aoki, G. Endrodi, Z. Fodor, S. D. Katz and K. K. Szabo, *Nature* **443**, 675-678 (2006)
 - [4] S. Ejiri, *Phys. Rev. D* **78**, 074507 (2008)
 - [5] E. S. Bowman and J. I. Kapusta, *Phys. Rev. C* **79**, 015202 (2009)
 - [6] P. Braun-Munzinger and J. Stachel, *Nature* **448**, 302-309 (2007)
 - [7] M. A. Stephanov, K. Rajagopal and E. V. Shuryak, *Phys. Rev. D* **60**, 114028 (1999)
 - [8] M. A. Stephanov, *Phys. Rev. Lett.* **102**, 032301 (2009)
 - [9] M. A. Stephanov, *Phys. Rev. Lett.* **107**, 052301 (2011)
 - [10] M. Asakawa, S. Ejiri and M. Kitazawa, *Phys. Rev. Lett.* **103**, 262301 (2009)
 - [11] See Supplemental Material at [LINK] for definition of cumulants and K-statistics, Two-Component Model calculation, significance calculation, magnified version of model calculations, statistics dependence of C_6/C_2 at 7.7 GeV, measurements with rapidity window $-0.5 < y < 0$.
 - [12] R. V. Gavai and S. Gupta, *Phys. Lett. B* **696**, 459-463 (2011)
 - [13] S. Gupta, X. Luo, B. Mohanty, H. G. Ritter and N. Xu, *Science* **332**, 1525-1528 (2011)
 - [14] F. Karsch and K. Redlich, *Phys. Lett. B* **695**, 136-142 (2011)
 - [15] P. Garg, D. K. Mishra, P. K. Netrakanti, B. Mohanty, A. K. Mohanty, B. K. Singh and N. Xu, *Phys. Lett. B* **726**, 691-696 (2013)
 - [16] S. Gupta, D. Mallick, D. K. Mishra, B. Mohanty and N. Xu, *Phys. Lett. B* **829**, 137021 (2022)
 - [17] M. M. Aggarwal *et al.* (STAR Collaboration), *Phys. Rev. Lett.* **105**, 022302 (2010)
 - [18] L. Adamczyk *et al.* (STAR Collaboration), *Phys. Rev. Lett.* **112**, 032302 (2014)
 - [19] J. Adam *et al.* (STAR Collaboration), *Phys. Rev. Lett.* **126**, 092301 (2021)
 - [20] M. Abdallah *et al.* (STAR Collaboration), *Phys. Rev. C* **104**, no.2, 024902 (2021)

- [21] L. Adamczyk *et al.* (STAR Collaboration), Phys. Lett. B **785**, 551-560 (2018) 546
547
- [22] L. Adamczyk *et al.* (STAR Collaboration), Phys. Rev. Lett. **113**, 092301 (2014) 548
549
- [23] J. Adam *et al.* (STAR Collaboration), Phys. Rev. C **102**, no.2, 024903 (2020) 550
551
- [24] A. Pandav, D. Mallick and B. Mohanty, Prog. Part. Nucl. Phys. **125**, 103960 (2022) 552
553
- [25] J. Adamczewski-Musch *et al.* [HADES], Phys. Rev. C **102**, no.2, 024914 (2020) 554
555
- [26] A. Bazavov, D. Bollweg, H. T. Ding, P. Enns, J. Goswami, P. Hegde, O. Kaczmarek, F. Karsch, R. Larsen and S. Mukherjee, *et al.* Phys. Rev. D **101**, no.7, 074502 (2020) 556
557
558
559
- [27] W. j. Fu, X. Luo, J. M. Pawlowski, F. Rennecke, R. Wen and S. Yin, Phys. Rev. D **104**, no.9, 094047 (2021) 560
561
- [28] M. Bleicher, E. Zabrodin, C. Spieles, S. A. Bass, C. Ernst, S. Soff, L. Bravina, M. Belkacem, H. Webers and H. Stoecker, *et al.* J. Phys. G **25**, 1859-1896 (1999) 562
563
564
- [29] S. Borsanyi, Z. Fodor, J. N. Guenther, S. K. Katz, K. K. Szabo, A. Pasztor, I. Portillo and C. Ratti, JHEP **10**, 205 (2018) 565
566
567
- [30] A. Bzdak and V. Koch, Phys. Rev. C **100**, no.5, 051902 (2019) 568
569
- [31] B. Ling and M. A. Stephanov, Phys. Rev. C **93**, no.3, 034915 (2016) 570
571
- [32] A. Bzdak, V. Koch, D. Oliinychenko and J. Steinheimer, Phys. Rev. C **98**, no.5, 054901 (2018) 572
573
- [33] M. Abdallah *et al.* (STAR Collaboration), Phys. Rev. Lett. **127**, 262301 (2021) 574
575
- [34] C. Adler, A. Denisov, E. Garcia, M. J. Murray, H. Strobele and S. N. White, Nucl. Instrum. Meth. A **470**, 488-499 (2001) 576
577
578
- [35] W. J. Llope, F. Geurts, J. W. Mitchell, Z. Liu, N. Adams, G. Eppley, D. Keane, J. Li, F. Liu and L. Liu, *et al.* Nucl. Instrum. Meth. A **522**, 252-273 (2004) 579
580
581
582
583
584
585
- [36] L. Adamczyk *et al.* (STAR Collaboration), Phys. Rev. C **96**, no.4, 044904 (2017)
- [37] K. H. Ackermann *et al.* (STAR Collaboration), Nucl. Instrum. Meth. A **499**, 624-632 (2003)
- [38] H. Bichsel, Nucl. Instrum. Meth. A **562**, 154-197 (2006)
- [39] Y. Zhang, Y. Huang, T. Nonaka and X. Luo, Nucl. Instrum. Meth. A **1026**, 166246 (2022)
- [40] M. S. Abdallah *et al.* (STAR Collaboration), Phys. Rev. Lett. **128**, 202303 (2022)
- [41] A. Bzdak and V. Koch, Phys. Rev. C **86**, 044904 (2012)
- [42] M. Kitazawa and M. Asakawa, Phys. Rev. C **86**, 024904 (2012) [erratum: Phys. Rev. C **86**, 069902 (2012)]
- [43] X. Luo, Phys. Rev. C **91**, no.3, 034907 (2015) [erratum: Phys. Rev. C **94**, no.5, 059901 (2016)]
- [44] A. Bzdak and V. Koch, Phys. Rev. C **91**, no.2, 027901 (2015)
- [45] M. Kitazawa, Phys. Rev. C **93**, no.4, 044911 (2016)
- [46] T. Nonaka, M. Kitazawa and S. Esumi, Phys. Rev. C **95**, no.6, 064912 (2017) [erratum: Phys. Rev. C **103**, no.2, 029901 (2021)]
- [47] X. Luo and T. Nonaka, Phys. Rev. C **99**, no.4, 044917 (2019)
- [48] X. Luo, J. Xu, B. Mohanty and N. Xu, J. Phys. G **40**, 105104 (2013)
- [49] T. Sugiura, T. Nonaka and S. Esumi, Phys. Rev. C **100**, no.4, 044904 (2019)
- [50] B. Efron, Annals Statist. **7**, no.1, 1-26 (1979)
- [51] A. Pandav, D. Mallick and B. Mohanty, Nucl. Phys. A **991**, 121608 (2019)
- [52] P. Braun-Munzinger, B. Friman, K. Redlich, A. Rustamov and J. Stachel, Nucl. Phys. A **1008**, 122141 (2021)
- [53] V. Vovchenko, V. Koch and C. Shen, Phys. Rev. C **105**, no.1, 014904 (2022)
- [54] R. Fisher, Proceedings of the London Mathematical Society s2-30, no.1, 198-238 (1930)